Additively Manufactured Profiled Conical Horn Antenna With Dielectric Loading

Shiyu Zhang, Darren Cadman, and John Yiannis Costas Vardaxoglou, *Fellow, IEEE*

***Abstract*—The world's first additively manufactured dielectric loaded profiled conical horn antenna is presented in this letter. With a smooth profiled flare and two loaded dielectric core materials, this horn offers symmetrical patterns, wideband gain, low sidelobe level, and low cross polarization. Additive manufacturing, including electroplating, has been employed to address the fabrication challenges. The measurement results show that the fabrication process produces a horn antenna with reduced mass and volume (<200 g with three-dimensional-printed flange) and high antenna performance with realized gain 16–20 dBi, sidelobe level −22 to −19 dB across the frequency range from 9 to 15 GHz.**

***Index Terms*—Antenna, additive manufacturing (AM), compact horns, dielectric loading, smooth profiled horn antenna, three-dimensional (3-D) printing.**

I. Introduction

A HORN antenna can take advantage of a smooth profile and dielectric materials loaded core to realize low sidelobes, excellent beam symmetry, and low cross polarization over the frequency range [1]–[4]. Compared with corrugated horns, the profiled horns have shorter length and reduced weight. They can be used in antenna systems that prefer small mass and volume such as reflector systems that require a compact feed design. However, the manufacturing of the traditional profiled horns and corrugated horns are usually carried out by using the computer numerical control machining that removes the metal from a bulk material. Rolland *et al.* [5] have reported a shaped horn that was micromachined from a bulk low-permittivity foam material and a metalized outer surface.

Additive manufacturing (AM) technology deposits successive layers of materials to create three-dimensional (3-D) objects. It has gathered immense attention from many applications including electromagnetics (EM) [6]–[9]. AM allows arbitrary geometries and internal structures that are difficult to realize by using traditional manufacturing techniques. For microwave applications, composite structures with a desired set of properties over a wide range of frequencies can be constructed [10], [11]. These structures could be viewed as artificial dielectrics and provide a means of altering the EM properties offering extra design freedom of materials for radio frequency circuits and components.

Manuscript received July 5, 2018; revised August 9, 2018 and August 27, 2018; accepted September 11, 2018. Date of publication September 20, 2018; date of current version October 26, 2018. This work was supported by UK's Engineering and Physical Science Research Council under the project "Synthesizing 3D Metamaterials for RF, Microwave and THz Applications" under Grant EP/N010493/1. *(Corresponding author: Shiyu Zhang.)*

The authors are with the Wolfson School of Mechanical, Electrical and Manufacturing Engineering, Loughborough University, Loughborough LE11 3TU, U.K. (e-mail: S.Zhang@lboro.ac.uk; D.A.Cadman@lboro.ac.uk; J.C. Vardaxoglou@lboro.ac.uk).

Digital Object Identifier 10.1109/LAWP.2018.2871029

Fig. 1. Photograph of additively manufactured profiled horn with dielectric loading after electroplating.

This letter presents the world's first conical horn antenna that has a smooth sinusoidal profile with two synthetic dielectric materials loaded in the core all realized by AM processes. The dielectric loading is used to improve pattern symmetry and provides good cross-polarization performance. The inner dielectric core transitions to the metal edge of the flare through an outer layer with lower dielectric constant, which results in exciting the hybrid HE_{11} mode, reported in theory only [12]. The two dielectric cores are concentric with the outermost metal shell and they all have the same profiles, as shown in Fig. 1. It is challenging to fabricate such a horn with a heterogeneous dielectric core by using a single process traditional manufacturing technique, particularly for the outer dielectric shell due to its low dielectric constant. Furthermore, the required dielectric materials may not be readily available off the shelf. To the best knowledge of the authors, a fabricated profiled horn antenna with dielectric loading has not been previously shown in the literature. With the advent of AM, artificial dielectrics with locally bespoke dielectric constants can be fabricated in a single process without multiple manufacturing [10], [13]. Assisted by metal plating of the outer surface, this profile horn antenna can be rapidly but inexpensively prototyped in house. This takes the design from a concept to a finished demonstrator in days.

II. Profiled Horn Design

The sinusoidal profiles of the horn can be described as follows [14]:

$$a(z) = \frac{D_g}{2} + \left(\frac{D_f}{2} - \frac{D_g}{2}\right)\left[(1-A)\frac{z}{L_f} + A\sin^2\left(\frac{\pi z}{4L_f}\right)\right] \quad (1)$$

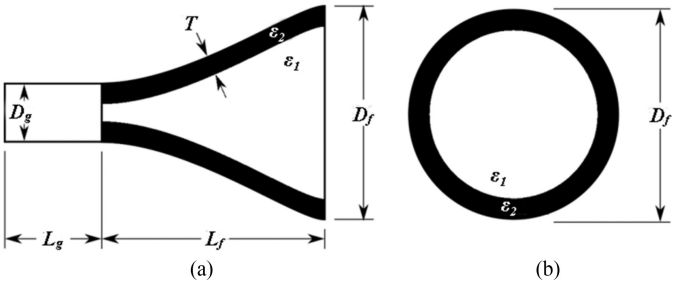

Fig. 2. Sketches of the proposed smooth profiled conical horn antenna. (a) Side view. (b) Front view.

TABLE I
DESIGN PARAMETERS OF THE PROFILED HORN ANTENNA

Name	Description	Value
D_g	Waveguide diameter	20.27 mm
L_g	Waveguide length	29.98 mm
D_f	Flare diameter	87.61 mm
L_f	Length of the flare	138.30 mm
T	Thickness of the outer dielectric layer	4.00 mm
ε_1	Relative permittivity of the core material	1.60
ε_2	Relative permittivity of the outer dielectric layer	1.06

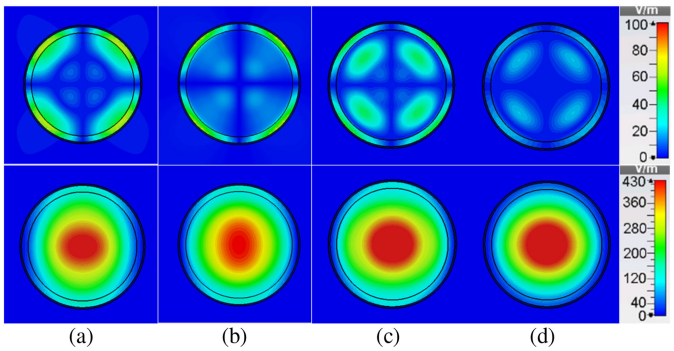

Fig. 3. Simulated electric field (top: *x*-component, bottom: *y*-component) of the profiled horn at (a) 9 GHz, (b) 11 GHz, (c) 13 GHz, and (d) 15 GHz.

where D_g is the diameter of the circular waveguide feed, D_f is the flare diameter of the open aperture, L_f is the total length of the horn, and A is the amount of profile added to a linear taper. The design sketch is shown in Fig. 2. As it is shown in Fig. 1, the horn comprises a circular waveguide, and has a profiled flare filled with dielectric loading that is composed of two parts: an inner core and an outer shell that have permittivity of ε_1 and ε_2, respectively ($\varepsilon_1 > \varepsilon_2$). The choice of parameters depends on the particular application. For the proof of concept, the parameters were optimized to excite the right hybrid HE_{11} mode and low sidelobes by using Antenna Magus with CST Microwave Studio. The design parameters are shown in Table I. In the simulation, the dielectric loading was modeled as homogenous dielectrics for reducing the computational complexity but without sacrificing the simulation accuracy. This approach has been applied to simulating graded index lenses [10]. The simulated electric field at the horn aperture is shown in Fig. 3. The horn axis was the *z*-axis of the electric field plot; therefore, it had *y*-axis as the *E*-plane, and *x*-axis as *H*-plane of the horn, respectively. In theory, the electric field should be dominated by the *y*-component to produce minimum cross-polarization level. Fig. 3 clearly shows that the hybrid mode HE_{11} has been excited across a wide frequency band. Simulation showed that the cross polarization was majorly contributed from the *x*-component and the theoretical cross-polarization level of this horn was below than -80 dB from 9 to 15 GHz.

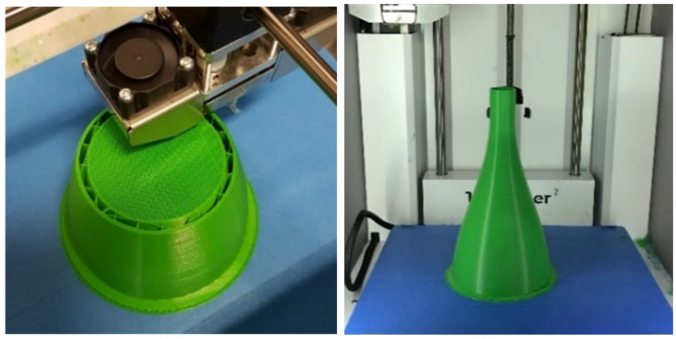

Fig. 4. (a) Photograph of halfway through the fabricating the nonsolid dielectric loading structure. (b) Finished profiled horn before metallization.

III. FABRICATING PROCESS

A. AM Dielectric Cores

In this letter, polylactic acid (PLA) that had relative permittivity $\varepsilon_r = 2.72$ was used to fabricated both dielectric core and shell. Any desired ε_r between 1 and 2.72 could be realized by creating nonsolid internal structures with air inclusions. The volume fraction of the nonsolid structure can be determined by using (1) [10]

$$f = \frac{\varepsilon_{\text{reff}} - 1}{\varepsilon_r - 1} \tag{2}$$

where f is the volume fraction of the dielectric material, $\varepsilon_{\text{reff}}$ is the expected effective relative permittivity of the nonsolid structure, and ε_r is the expected effective relative permittivity of the solid dielectric material. Both dielectric loss and total mass can be reduced due to the air voids in the nonsolid structures, which will benefit the horn performance.

A low-cost desktop 3-D printer Ultimaker 2+ was used to fabricate the dielectric loaded profiled horn. To achieve a smooth-walled profile, thin layer height (0.05 mm) and fine nozzle (0.25 mm) were used. Fig. 4(a) shows the photograph of manufacturing when the shell and core were fabricated halfway through, where the dielectric core and the shell having different infill factors. The entire dielectric loading was fabricated in a single process without assembly.

Fig. 5 shows the top view of the flare side of the horn. It shows that the infills are composed of grid lines that results from slicer software setting. The grid size of the inner dielectric core was approximately 0.5 mm. As the electric field of this horn was propagated along the horn axis, the grid infill provided uniform distribution on the plane that is normal to the electric field. The partially infilled structures formed artificial dielectrics to provide the bespoke permittivity values.

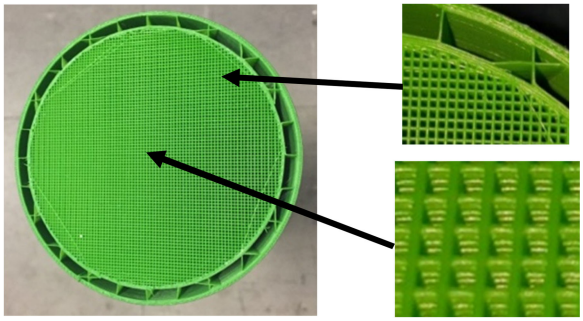

Fig. 5. Photograph of top view of the horn when looking from the flare side.

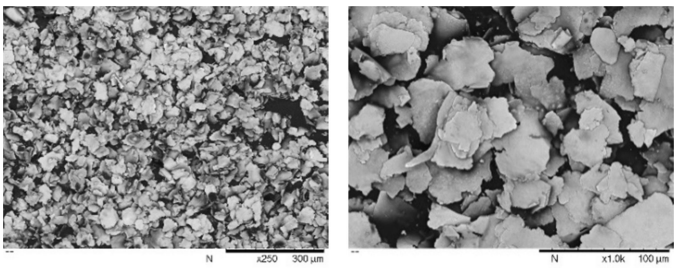

Fig. 6. SEM images of conductive surface after copper coating. (a) Zoomed in 250 times. (b) Zoomed in 1000 times.

B. Electroplating

After the two dielectric cores were created, the outer surface was metal-plated by using conductive spray with the electrical surface resistance of 0.1 Ω/sq. A circular X-band waveguide flange was also 3-D-printed and metalized to connect this horn to a standard circular waveguide feed.

The conductivity of the outer surface offered by the conductive spray was then enhanced through copper (Cu) plating. A target Cu thickness of approximately more than 10 skin depths ($\sim$10 μm) was aimed for. During electroplating, the current supplied to the profiled horn antenna in the plating solution was limited to less than 2 mA for an hour to provide an initial foundation layer of Cu. Once the foundation layer had been deposited, the current was increased to accelerate the Cu deposition. This process took approximately more than 5 h time for rinsing in water. The visual appearance of the plated horn became tarnished over time due to residual copper sulphate ($CuSO_4$) leaching out of the layers of the AM structure. This could be mitigated through optional and additional rinsing stages. The scanning electron microscope (SEM) images of the conductive surface are shown in Fig. 6. It shows that the PLA surface is well covered by the microconductive particles after multiple-layer coating.

The surface topography of the coated horn antenna was investigated by using a Talysurf CLI 2000 (Taylor Hobson Ltd., Leicester, U.K.), a high-resolution surface profiling system. The surface profile of the horn over a 20-mm distance is shown in Fig. 7. The average total height of the surface profile (the distance from the deepest valley to the highest peak) was approximately 76.1 μm. The surface roughness Ra (arithmetic mean deviation of the roughness profile) was measured at eight random positions on the conductive surface and the average value was 8.050 μm with standing error of 0.403 μm.

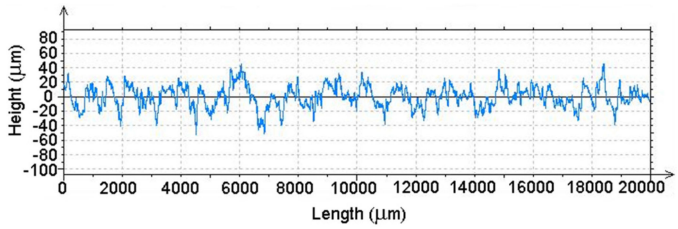

Fig. 7. Surface profile of the metallized surface.

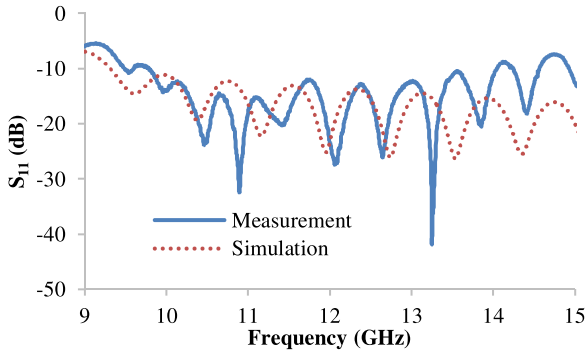

Fig. 8. Measured S_{11} results of the profiled horn antenna.

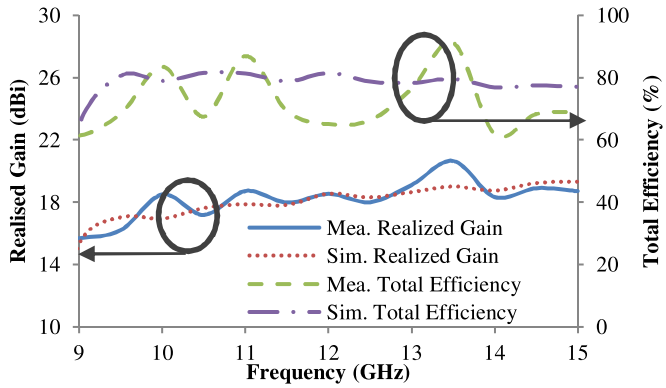

Fig. 9. Measured and simulated gain and efficiency of the synthetic dielectric loaded profiled horn.

IV. Measured Results

The dielectric loaded profiled horn with the 3-D-printed flange was connected to a standard circular waveguide and measured in the anechoic chamber at Loughborough University. The measured S_{11} is shown in Fig. 8, and it is below -10 dB from 10 to 14 GHz. Outside this frequency band, greater mismatch is observed. The measurement realized gain at the boresight and total efficiency (includes return loss) are shown in Fig. 9, compared with CST full wave simulation. It shows that the profiled horn antenna offers 16.0–20.0 dBi gain and 60–91% total efficiency over the frequency range from 9 to 15 GHz. Note that, at some frequency points, the measured efficiency was lower than the simulation, whereas the measured gain was higher than the simulation. This was due to measurement error causing a variation in the final results. The aperture efficiency of this profiled horn was from 46% to 75% over the frequency range.

Fig. 10 shows the measured radiation patterns at 9, 11, 13, and 15 GHz, compared with the CST simulated results. It shows good agreement between simulation and measurement. The

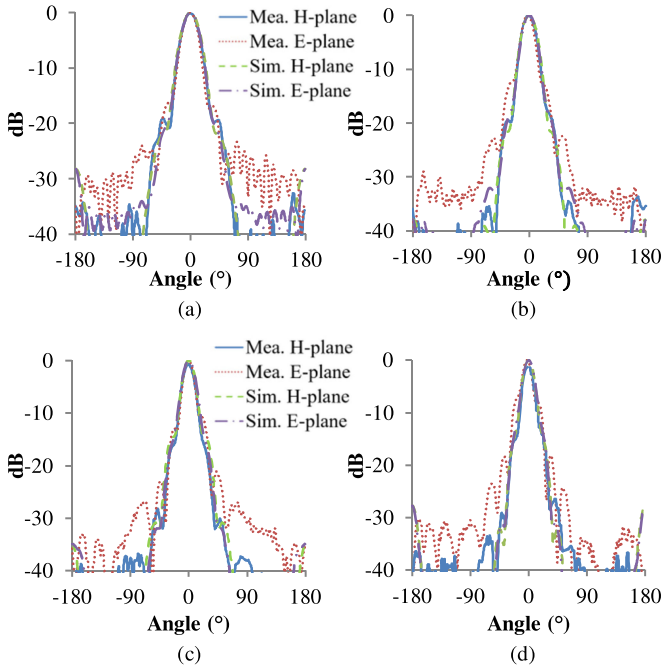

Fig. 10. Measured and simulated *H*-plane and *E*-plane radiation patterns of the profiled horn at (a) 9 GHz, (b) 11 GHz, (c) 13 GHz, and (d) 15 GHz.

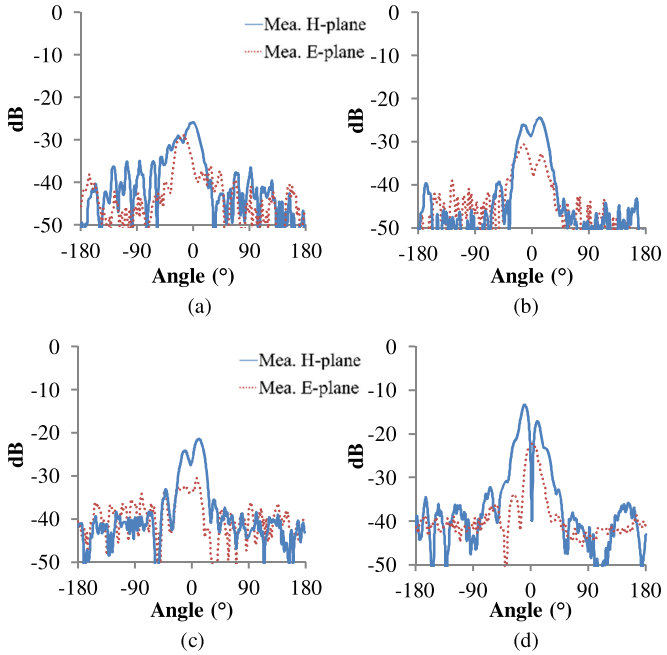

Fig. 11. Measured *H*-plane and *E*-plane cross-polarization patterns of the profiled horn at (a) 9 GHz, (b) 11 GHz, (c) 13 GHz, and (d) 15 GHz.

profiled horn produced symmetrical patterns around the boresight axis, and low sidelobe level (less than −22 dB) was observed at 11 and 13 GHz, but it was increased to −19 dB at 9 and 15 GHz. High directive beam was observed across the frequency range, and the 3 dB beamwidth ranged from 17° to 26° as the frequency reduced.

The measured cross-polarization patterns are shown in Fig. 11, showing good polarization performance of this 3-D-printed antenna with cross-polarization levels below −22 dB confirming the HE_{11} mode is dominant. However, the cross-polarization level increased at 15 GHz mainly due to the dielectric constant variations in the inner part that gave rise to the cross polar components, which affected the purity of the balanced mode or hybrid mode.

TABLE II
COMPARISON OF HORN ANTENNAS RADIATION PERFORMANCE

Name	Length (mm)	3dB beamwidth E(H) plane (deg)	Aperture efficiency (%)	Peak cross-polar level (dB)
Linear conical horn, no dielectric loading (simulated)	138	16.8 (20.9)	71.8	-17.2
Profiled horn, no dielectric loading (simulated)	138	16.4 (19.5)	75.1	-18.5
Profiled horn from [1] (theoretical value)	150	16.1 (16.1)	32.0	-27.5
Additively manufactured profiled horn (simulated)	138	19.0 (19.0)	75.0	-29.3

A comparison of the radiation performance of horn antennas is shown in Table II. The conventional linear conical horn and the profiled horn had the same aperture size and total length that the AM horn had but without dielectric loading. The antenna performance of the conventional horns was simulated by using CST. Table II shows that profiling a horn with dielectric loading can significantly improve the beam symmetry and cross polarization. Table II also includes the profiled horn from [1] for comparison. Note that the horn in [1] was only shown in theory and was not manufactured. The AM horn here is the first dielectric loaded profiled horn that has been fabricated and measured.

V. CONCLUSION

This letter has demonstrated a novel approach of rapidly fabricating the world's first low-cost and lightweight smooth profiled horn antenna with heterogeneous dielectric loading. The two different dielectric materials with the desired sinusoidal profiles have been fabricated by using a single process AM technique. The two dielectrics were fabricated as nonsolid structures. The air voids in the structures not only reduced the dielectric loss but also reduced the mass of the horn significantly. After fabricating the dielectric loading, electroplating created the outer conductive shell. The total weight of this horn including a 3-D-printed flange was 198.1 g.

The measured results showed that this profiled horn offered wideband gain from 16.0 to 20.0 dBi at the frequency range from 9 to 15 GHz with aperture efficiency from 46% to 75%. Boresight axis symmetry radiation patterns were observed, with low sidelobe level −22 to −19 dB across the entire frequency range and cross-polarization level less than −21 dB up to 13 GHz. This rapid prototyping concept shows that AM is ideal for fabricating various horn feed systems offering design freedom and shortened lead time.

ACKNOWLEDGMENT

The authors would like to thank Dr. W. Whittow for valuable discussions of this work and thank Dr. T. Goulas for helping with the SEM image and surface roughness analysis.

REFERENCES

[1] A. Olver and B. Philips, "Profiled dielectric loaded horns," in *Proc. 8th Int. Conf. Antennas Propag.*, 1993, no. 2, pp. 788–791.

[2] C. Granet, R. Bolton, and G. Moorey, "A smooth-walled spline-profile horn as an alternative to the corrugated horn for wide band millimeter-wave applications," *IEEE Trans. Antennas Propag.*, vol. 52, no. 3, pp. 848–854, Mar. 2004.

[3] J. M. Gil, J. Monge, J. Rubio, and J. Zapata, "A CAD-oriented method to analyze and design radiating structures based on bodies of revolution by using finite elements and generalized scattering matrix," *IEEE Trans. Antennas Propag.*, vol. 54, no. 3, pp. 899–907, Mar. 2006.

[4] R. Cahill, "Design of core support mechanism for mm-wave dielectrically loaded horn," *Electron. Lett.*, vol. 25, no. 18, pp. 1248–1249, 1989.

[5] A. Rolland, N. T. Nguyen, R. Sauleau, C. Person, and L. Le Coq, "Smooth-walled light-weight Ka-band shaped horn antennas in metallized foam," *IEEE Trans. Antennas Propag.*, vol. 60, no. 3, pp. 1245–1251, Mar. 2012.

[6] A. Bisognin *et al.*, "3D printed plastic 60 GHz lens: Enabling innovative millimeter wave antenna solution and system," in *Proc. IEEE MTT-S Int. Microw. Symp.*, 2014, pp. 1–4.

[7] C. R. Garcia *et al.*, "3D printing of anisotropic metamaterials," *Prog. Electromagn. Res. Lett.*, vol. 34, pp. 75–82, 2012.

[8] G. P. Le Sage, "3D printed waveguide slot array antennas," *IEEE Access*, vol. 4, pp. 1258–1265, 2016.

[9] G. Du, M. Liang, R. A. Sabory-Garcia, C. Liu, and H. Xin, "3-D printing implementation of an X-band eaton lens for beam deflection," *IEEE Antennas Wireless Propag. Lett.*, vol. 15, pp. 1487–1490, 2016.

[10] S. Zhang, R. K. Arya, S. Pandey, Y. Vardaxoglou, W. Whittow, and R. Mittra, "3D-printed planar graded index lenses," *IET Microw. Antennas Propag.*, vol. 10, no. 13, pp. 1411–1419, Oct. 2016.

[11] J. Tribe, W. G. Whittow, R. W. Kay, and J. C. Vardaxoglou, "Additively manufactured heterogeneous substrates for three-dimensional control of local permittivity," *Electron. Lett.*, vol. 50, no. 10, pp. 745–746, May 2014.

[12] B. Philips and A. D. Olver, "Design and performance of profiled dielectric loaded horns," *Proc. IEE—Microw. Antennas Propag.*, vol. 141, no. 5, pp. 337–341, 1994.

[13] M. Liang, W. Ng, K. Chang, K. Gbele, M. E. Gehm, and H. Xin, "A 3-D luneburg lens antenna fabricated by polymer jetting rapid prototyping," *IEEE Trans. Antennas Propag.*, vol. 62, no. 4, pp. 1799–1807, Apr. 2014.

[14] A. D. Olver and J. Xiang, "Design of profiled corrugated horns," *IEEE Trans. Antennas Propag.*, vol. 36, no. 7, pp. 936–940, Jul. 1988.